JCTC Journal of Chemical Theory and Computation

Semiempirical Molecular Orbital Scheme To Study Lanthanide(III) Complexes: PM3 Parameters for Europium, Gadolinium, and Ytterbium

Jonathan P. McNamara, Sean D. Berrigan, and Ian H. Hillier*

School of Chemistry, University of Manchester, Manchester M13 9PL, U.K.

Received October 12, 2006

Abstract: Semiempirical parameters for europium, gadolinium, and ytterbium have been developed for use in the PM3 method to allow the structure and energetics of complexes containing lanthanide(III) ions to be accurately modeled. At the semiempirical level, the lanthanide(III) ion is represented by a +3 core and has a minimal basis of 6*s*5*d*6*p* (9 atomic orbitals), the 4*f* electrons being included within the electronic core. Training sets containing up to 19 lanthanide complexes, with data computed at the density functional theory (DFT) level, have been employed for each lanthanide(III) ion. A gradient-based optimization algorithm has been used, and important modifications of the core repulsion function have been highlighted. The derived parameters lead in general to good predictions of the structure of the complexes and demonstrate improvements in the prediction of water binding energies compared to the AM1/sparkle model. For the 28 Eu(III), 28 Gd(III), and 29 Yb(III) complexes optimized at the DFT level, the PM3 average unsigned mean errors for all interatomic distances between the lanthanide(III) ion and the ligand atoms of the first coordination sphere are 0.04, 0.03, and 0.03 Å, respectively. The derived parameters are shown to be comparable to small-basis set DFT calculations in predicting the experimental structures of various lanthanide(III) complexes. The derived parameter sets provide a starting point should greater accuracy for a more restricted range of compounds be required.

Introduction

Since the late 1980s there has been an increasing interest in the physicochemical properties and reactivity of the lanthanide (Ln) elements, Ce ($Z = 58$) through to Lu ($Z = 71$) driven by their potential applications in photoluminescence[1−4] and medical imaging.[5−9] For example, Gd(III) complexes are currently used as "in vivo" magnetic resonance imaging (MRI) contrast agents which increase the contrast between diseased and normal tissue and/or show the status of organ function and blood flow by enhancing the water proton relaxation rate. Crucial to the design of such complexes is ensuring the complexing ligands form compounds with Gd(III) which possess high kinetic and thermodynamic stability, as the free ions are extremely toxic. As far as Gd(III) is concerned, the usual complexing ligands involve octadentate polyamino carboxylate (PAC) ligands such as DOTA (Chart 1).[10]

An understanding of the chemistry of the lanthanides is also of increasing importance in nuclear fuel reprocessing,[11,12] where the separation of nuclear wastes containing both trivalent lanthanides and trivalent minor actinides (e.g., Am(III) and Cm(III)] is complicated by the similar chemical properties of these species. The recent upsurge in lanthanide research activity has also been driven by an interest in the use of these complexes in light conversion molecular devices, such as luminescent materials[4] and antennae in photosensitive bioinorganic compounds.[8]

The use of quantum mechanical (QM) modeling is now well established for the understanding of structures and mechanisms involving the *d*-transition metal elements.[13−15] However, there are considerable challenges for the routine

* Corresponding author phone: +44 (0) 161 275 4686; fax: +44 (0) 161 275 4734; e-mail: Ian.Hillier@manchester.ac.uk.

10.1021/ct600304g CCC: $37.00
Published on Web 02/28/2007

Chart 1. Structure of the Gadolinium(III) DOTA Complex[10]

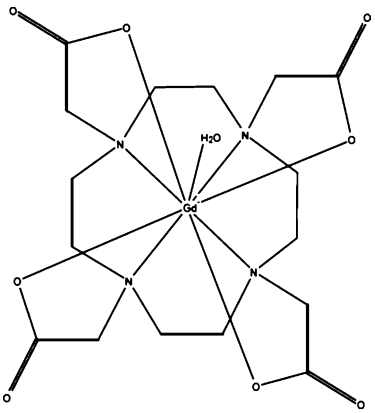

application of QM approaches to the heavier elements.[16] For these elements, all-electron studies are generally prohibitive due to the large number of orbitals and electrons (many of which are in the core) and the difficulties associated with the presence of open-shell 4*f* electrons. Moreover, as the periodic table is descended, relativistic effects and electron correlation become increasingly important. In addition the complexes of the heavier elements often involve high coordination numbers of the central metal atom and sterically bulky ligands (>50 atoms) which often prohibits the use of more established ab initio methods for their study.

At present most ab initio or density functional theory (DFT) calculations make use of relativistic effective core potentials (RECP) which treat only the heavy element valence electrons and incorporate relativistic effects into the core, thus reducing the computational effort.[17] Within this approach the 4*f* electrons may or may not be included within the electronic core giving the so-called "large" or "small" core approach. Calculations of $Ln(NR_2)_3$ (R = H or SiH_3) at the DFT level using both large and small core RECPs indicate accurate models can be obtained by including the 4*f* electrons within the electronic core.[18]

To date there have been a number of high-level ab initio calculations reported on quite small lanthanide complexes. Cao and Dolg have calculated the third and fourth ionization energies of the lanthanide atoms (La to Lu) using the CASSCF method[19] and have also used ab initio methods to study open-shell lanthanide dimers (Ce_2, Pr_2, and Gd_2)[20] and the lanthanum monohalides.[21] Takeda et al. have reported stabilities of the hexafluoride anions of the lanthanides, LnF_6^{2-} and LnF_6^{3-} (Ln = Ce to Lu) at the CASSCF/RECP level.[22] For larger complexes, such as $[Ln(DOTA)(H_2O)]^{1-}$, the Hartree−Fock (HF) method with a relatively small 3-21G basis set has been shown to give quite good predictions of the structure of these complexes.[16,23,24]

More recently, DFT has been the method of choice for including electron correlation in calculations of quite large lanthanide complexes. Cosentino et al. have reported calculations of $[Gd(H_2O)_9]^{3+}$ at the HF, DFT, and MP2 levels using a 3-21G basis set for the ligand atoms and found the results to be in qualitative agreement with those obtained using larger basis sets including polarization functions.[24] Similarly, Smentek et al. have reported calculations of a series of lanthanide DOTA complexes which are in good agreement with both experimental structural and energetic data.[25] DFT calculations showing good agreement between theory and experiment have also been reported for $Ln(dpm)_3$ (Ln = La, Nd, Gd, Er, Yb, Ly; dpm = dipivoloymethanoate),[26] $[Ln(H_2O)_9]^{3+}$ (Ln = La, Eu, Lu), and structures involving the 2,2′:6′,2″-terpyridine[27] and the texaphyrin ligands.[28] DFT methods have also been used to calculate the structures and bond strengths of the lanthanide halides, the results of which have been shown to be in good agreement with high-level CCSD(T) calculations.[29]

Due to the difficulties in modeling lanthanide complexes a number of researchers have turned to the use of molecular mechanics (MM) methods for structure prediction.[30,31] The use of MM techniques for studying *f*-block elements is sometimes problematic due to the scarcity of data for parametrization. Villa et al. fitted an empirical potential to HF calculations of $[Gd(THP)OH_2]^{3+}$, $[Gd(TMA)(OH_2)]^{3+}$, and $[Gd(DOTMP)]^{1-}$ and were able to extend the use of the empirical parameters to study other gadolinium containing complexes.[16,32] Consentino et al. also parametrized their MM potentials against ab initio calculations and found the quality of the parameters depended strongly on the level at which the potential energy surface was calculated.[33] Moreover, Kowall et al. have also developed potentials (including polarization) that were fitted to ab initio calculation in order to better describe Ln^{3+}−water interactions (Ln = Nd, Sm, Yb). These potentials were then used in classical molecular dynamics (MD) simulations to understand water exchange at tripositive lanthanide ions.[34] Importantly, the calculated coordination numbers of the lanthanide ions and the water exchange rate constants were found to be consistent with experimental data. More recently, van Veggel and Reinhoudt have developed Lennard-Jones parameters for La^{3+}, Nd^{3+}, Gd^{3+}, and Yb^{3+} which correctly predict the experimental free energies of hydration of these ions. In addition, these calculations, using a TIP3P water model, also yield radial distribution functions for each lanthanide ion in good agreement with the available experimental data.[35]

However, in spite of advances in modern computation hardware and the development of DFT methods and multilevel modeling schemes (e.g., QM/MM[36,37] and ONIOM[38]), the computational study of lanthanide chemistry is still at the limit of computational feasibility. For this reason, in this and other areas of condensed phase modeling there has been a renaissance in the use of semiempirical molecular orbital (MO) methods. For example, we[39] and others[40] have successfully quantified the extreme tunneling in the enzyme methylamine dehydrogenase (MADH) using a QM/MM potential and variational transition state theory combined with semiclassical tunneling corrections. To achieve the necessary accuracy, a reparametrization of the PM3 Hamiltonian was required. The use of such specific reaction parameters (SRP), first suggested by Rossi and Truhlar,[41] is central to the continuing successful exploitation of these semiempirical methods.

At present the majority of semiempirical methods (MNDO, AM1, and PM3) are based upon the NDDO approximation and have been widely applied to the study of systems containing the main group elements.[42−44] These methods have

recently been extended[45] so that all the nonradioactive main group elements (excluding the noble gases) can now be treated using such techniques and have, in some instances, been extended to include *d*-orbitals. Thiel and Voityuk have proposed an extension of the MNDO method to include *d*-orbitals, MNDO/d, which has been successful in describing hypervalent compounds of the main group elements where *d*-orbitals are important.[46,47] As far as transition-metal atoms are concerned we have been developing a parametrization strategy to allow the PM3 method to be used to study iron-containing proteins, focusing on iron-sulfur, iron-heme, and iron-only hydrogenases.[48−51] The development of parameters for lanthanide elements is likely to be particularly challenging given the difficulties in accounting for the 4*f* electrons and relativistic effects and due to the size of the complexing ligands (>50 atoms).

There has, however, been some progress in the development of semiempirical methods to treat the heavy elements. Culberson et al. has used the INDO method to examine the electronic structure of a series of lanthanide complexes and found the 4*f* orbitals were required for the halides but were less important for the high coordination complexes.[52] Kotzian and co-workers have also used the INDO/S-CI method (including spin−orbit coupling), to study a range of lanthanide monoxide complexes.[53−55]

In recent years, significant progress has been made with the development of the so-called sparkle model for treating lanthanide atoms. The success of the sparkle approach is based upon the assumption that most Ln−ligand bonds are essentially electrostatic in nature and the lanthanide 4*f* orbitals do not make a significant contribution to the bonding. Sparkles were originally introduced as part of the MOPAC semiempirical package and were designed to represent pure ionic charges.[56] They can be visualized as essentially a charge delocalized over the surface of a sphere, with an ionic radius of 0.7 Å, integer nuclear charges (+2, +1, −1, or −2 depending on the entity they represent), zero heat of atomization, no orbitals, and no ionization potential.[57] Crucially they are unable to donate or accept electrons. In the case of a lanthanide atom, the sparkle model involves a nuclear charge of +3, the most commonly encountered oxidation state across the series.

In 1994 the first sparkle model (within the AM1 scheme) for lanthanide complexes (SMLC) was reported for Eu(III), and the parameters were fitted to reproduce the structure of a single Eu(III) complex, $[Eu(acac)_3.o\text{-phen}]$.[58] This model yielded Eu−ligand distances with an average Eu−ligand deviation of 0.36 Å (from experiment) which was later refined to 0.20 Å by the inclusion of two spherical Gaussian functions in the core repulsion term.[59] More recently, the SMLCII model for Eu(III) was developed which improved on the early revision by increasing the size of the training set from a single Eu(III) complex to one which included 15 complexes spanning a range of ligand environments.[60] This approach led to a significant improvement in the prediction of experimental structures for the 96 tested complexes [deviation from experiment for Ln−ligand bonds, 0.68 Å (SMLC), 0.28 (SMLCII), and 0.09 Å (most recent)]. The AM1 sparkle model (AM1/SMLCII) has since been extended to nearly all lanthanide(III) elements by fitting to complexes available in the Cambridge Structural Database (CSD).[61] To date AM1/sparkle parameters are available for Gd and Tb;[60] Pm and Sm;[62] Yb;[63] La and Lu;[64] Dy;[65] Pr;[66] Nd;[67] and Er and Ce.[68] Very recently the Tm(III) sparkle model has been reported for use within the PM3 semiempirical scheme.[69] Both the AM1 and PM3 sparkle implementations have been extensively tested and are certainly capable of predicting structures quite close to experiment for high coordination complexes.

However, what is less clear is whether this approach is capable of describing energetic processes (e.g., the binding energy of water in $[Gd(DOTA)(OH_2)]^{1-}$ important in developing new MRI contrast agents) or those lanthanide complexes where covalent effects may be "non-negligible" and the presence of the orbitals centered on the lanthanide atom are important.

Developing the Semiempirical Model

1. Improving the Semiempirical Sparkle Model. The success of the sparkle model is based on the assumption that lanthanide(III) ions behave like simple ions. The open-shell 4*f* orbitals are shielded from external fields outside the nucleus by the closed-shell 5*s* and 5*p* electrons. Thus the effect of the 4*f* orbitals is often assumed to be small, much in the same way as DFT or ab initio calculations using "large" core RECPs assume a negligible contribution from the 4*f* orbitals to the Ln−ligand bonding.[18] However, the sparkle model does assume *complete* ionization of the valence electrons, and therefore covalent effects cannot be included.[60] Freire et al. have suggested that covalent effects could be accounted for by including *s* and *p* valence orbitals on the sparkle +3 metal center.[60] In our work we have chosen to augment the AM1/sparkle model for lanthanides by adding 6*s*, 5*d*, and 6*p* orbitals to the valence basis and account for the 4*f* electrons as part of the electronic core, in line with "large" core RECP calculations.[18] Thus each lanthanide atom has a core charge of +3 and 6*s*, 5*d*, and 6*p* valence atomic orbitals. We have chosen to implement our orbital-based sparkle model within the PM3 framework.[44]

2. Modification of the Core Repulsion Function. Within the NDDO approximation, the core−electron attraction ($V_{\mu\nu,B}$) and core−core repulsion (E_{AB}^{MNDO}) are usually expressed in terms of two-center two-electron integrals (eqs 1 and 2) where Z_A and Z_B correspond to the core charges, R_{AB} is the internuclear separation, and α_A and α_B are adjustable parameters.[42]

$$V_{\mu\nu,B} = -Z_B(\mu^A\nu^A,s^Bs^B) \quad (1)$$

$$E_{AB}^{MNDO} = Z_AZ_B(s^As^A,s^Bs^B)(1 + e^{-\alpha_A R_{AB}} + e^{-\alpha_B R_{AB}}) \quad (2)$$

The form of the core−electron attraction (eq 1) is common to all NDDO methods, while eq 2 gives the form of the core repulsion function used within the MNDO method.[42] The form of the core repulsion function in AM1 and PM3 differs from that used in MNDO in that an additional term involving one to four Gaussian functions (denoted *a*−*c*, eq 3) is also included.[43,44]

$$E_{AB}^{AM1,PM3} = E_{AB}^{MNDO} + \frac{Z_A Z_B}{R_{AB}} \sum_{i=1}^{4} [a_{iA} e^{-b_{iA}(R_{AB}-c_{iA})^2} + a_{iB} e^{-b_{iB}(R_{AB}-c_{iB})^2}] \quad (3)$$

For methods which include *d*-orbitals (e.g., MNDO/d and AM1/d),[46,47,70−72] it has been found that to obtain the correct balance between attractive and repulsive Coulomb interactions requires an additional adjustable parameter ρ (previously evaluated using the one-center two-electron integral, G_{ss}, eq 4), which is used in the evaluation of the two-center two-electron integrals used in these terms (eq 5):

$$\rho = \frac{1}{2G_{ss}} \quad (4)$$

$$(s^A s^A, s^B s^B) = \frac{e^2}{(R_{AB}^2 + (\rho_A + \rho_B)^2)^{1/2}} \quad (5)$$

However, in spite of these modifications, when applying these methods to the study of molybdenum complexes Voityuk and Rösch[70] found that use of the NDDO core repulsion function (eq 3) led to some systematic deviations for some Mo−X bond lengths. This led them to further modify the form of the core repulsion function for their AM1/d Hamiltonian by introducing bond specific parameters, α_{Mo-X} and δ_{Mo-X} (eq 6).

$$E_{Mo-X}^{AM1/d} = Z_{Mo} Z_X (s^A s^A, s^B s^B)[1 + 2\delta_{Mo-X} e^{-\alpha_{Mo-X} R_{Mo-X}}] \quad (6)$$

This modification was found to be more efficient than using Gaussian functions and has since been used in the extension of NDDO-based methods to the remaining main group elements and the AM1* parametrization of some second-row elements[71] and transition metals.[72] This is the form of the core repulsion function adopted here. Thus for each lanthanide (Eu, Gd, Yb) the PM3 Gaussian parameters *a*−*c* are set to zero, there is an additional adjustable parameter ρ, and for each Ln−X interaction there are separate α_{Ln-X} and δ_{Ln-X} parameters. In the AM1/d parametrization of molybdenum[70] and in our PM3 parametrization of iron,[51] the core repulsion function had to be modified in the case of atom X being hydrogen. We find that in our PM3 model for the lanthanides no such modifications are required. The form of our core repulsion function differs from that used in the sparkle model which is based on the original AM1 and PM3 core repulsion function (eq 3).[43,44]

Parametrization Strategy

1. Construction and Optimization of the Error Function. We here outline our developing strategy to obtain semiempirical parameters for the lanthanide metals, which follows closely our strategy used to obtain parameters for iron. A central feature, common to all optimization strategies, is the construction and subsequent minimization of the error function, *S*, eq 7

$$S = \sum_i w_i (q_i^{semiempirical} - q_i^{reference})^2 \quad (7)$$

where $q_i^{semiempirical}$ and $q_i^{reference}$ are the molecular quantities calculated at the semiempirical level and the corresponding reference values (usually from experiment or high-level calculation), and w_i is an appropriate weighting factor. The aim of any parameter optimization strategy is to minimize *S* efficiently and this can be achieved using either a genetic algorithm (GA)[41,48,49,73−76] or a gradient-based algorithm.[44,45,50,51] One of the central features of the work reported herein is the use of an efficient gradient-based optimization algorithm based upon a modified Broyden-Fletcher-Goldfarb-Shanno (BFGS) method.[44,45,77,78] Details of this algorithm and the modifications for obtaining semiempirical parameters for transition metals have been reported previously.[50,51] Therefore, our approach differs from the optimization of AM1/sparkle and PM3/sparkle parametrizations which used a combination of Newton−Raphson and simplex optimization methods.[60,63]

The chosen error function (*S*, eq 7; see also Table S1 and Figure S1) for each lanthanide element contained weighted contributions from the internal coordinate gradients for each reference complex and also the relative energy (calculated at the DFT level) of the $[Ln(DOTA)(OH_2)]^{1-}$ structures [the square antiprismatic isomer (A) and the inverted antiprismatic isomer (IA)]. Our parametrization strategy differs from that of the AM1/sparkle approach[60,63] in that our reference data include not only structural but also some energetic data.

2. Choice of Reference Data. Historically the reference data used in semiempirical parametrizations is obtained using a wide range of experimental techniques.[42−45,77,78] There is, however, a growing trend to replace some of the reference data with information obtained from high-level ab initio calculations (e.g., G2 or G3 methods) or, more recently, DFT calculations.[49−51,71,72] Such an approach is of increasing importance, particularly in the absence of experimental data or where the reliability of experimental data is questionable. Winget et al. have suggested that a semiempirical method, which behaved as well as, for example, B3LYP/6-31G*, would be a significant advance in this area.[71] For this reason, in our PM3 parametrization for iron[49−51,74] we chose to calculate all our reference data at the DFT (B3LYP)[79−81] level using a 6-31G* basis set, and this is also the approach adopted herein.

The reference data for europium, gadolinium, and ytterbium was obtained from DFT calculations at the B3LYP level, performed using the GAUSSIAN 98[82] and GAUSSIAN 03[83] suites of programs. Our choice of DFT functional is supported by the calculations of Heiberg et al. on a series of LnF complexes (Ln = Nd, Eu, Gd, Yb) where the B3LYP functional gave geometries and bond strengths in good agreement with CCSD(T) values.[29] The DFT calculations reported herein employed the 46 + 4*f* ^{n} electron RECP of Dolg et al., which treats the outermost 11 electrons explicitly, with valence ground configurations $5s^2 5p^6 6s^2 5d^1$ for the lanthanide atom and $5s^2 5p^6 6s^0 5d^0$ for the lanthanide(III) cation.[84] The remaining 46 + 4*f* ^{n} electrons are placed in the core. The 3-21G basis set was chosen for the ligand atoms as it has been found to give structures and conformational energies of $[Gd(H_2O)_9]^{3+}$ in qualitative agreement with those obtained using basis sets including polarization functions.[24]

Table 1. Bond Lengths (Å) and Bond Angles (deg) for the LnX_3 (X = H, CH_3, F, Cl, Br, NH_2) Complexes Calculated at the DFT,[a] AM1/Sparkle, and PM3 Levels of Theory

		average value		
ligand[b]		Eu	Gd	Yb
H				
distances	DFT	2.058	2.046	1.996
	PM3	1.996	2.018	2.041
	AM1/sparkle	1.003	0.837	0.814
angles	DFT	111.7 (0.0)	111.6 (0.1)	114.2 (0.0)
	PM3	103.1 (0.0)	106.0 (0.0)	110.5 (0.0)
	AM1/sparkle	120.0 (0.1)	120.0 (0.1)	120.0 (0.0)
CH_3				
distances	DFT	2.437	2.426	2.367
	PM3	2.393	2.425	2.433
	AM1/sparkle	2.040	2.093	2.096
angles	DFT	107.8 (0.1)	107.8 (0.0)	109.6 (0.0)
	PM3	110.8 (0.0)	113.3 (0.0)	116.0 (0.0)
	AM1/sparkle	120.0 (0.0)	120.0 (0.0)	120.0 (0.0)
F				
distances	DFT	2.073	2.063	2.006
	PM3	2.080	2.055	2.036
	AM1/sparkle	2.290	2.315	2.252
angles	DFT	115.5 (0.0)	116.3 (0.4)	118.9 (0.4)
	PM3	108.8 (0.0)	110.0 (0.0)	114.2 (0.0)
	AM1/sparkle	120.0 (0.0)	120.0 (0.0)	120.0 (0.0)
Cl				
distances	DFT	2.556	2.541	2.476
	PM3	2.524	2.524	2.480
	AM1/sparkle	2.308	2.333	2.265
angles	DFT	119.6 (0.7)	118.6 (0.9)	120.0 (0.3)
	PM3	106.2 (0.0)	108.6 (0.0)	120.0 (0.0)
	AM1/sparkle	120.0 (0.0)	120.0 (0.0)	120.0 (0.2)
Br				
distances	DFT	2.696	2.683	2.618
	PM3	2.601	2.671	2.610
	AM1/sparkle	2.299	2.323	2.259
angles	DFT	120.0 (0.0)	120.0 (0.0)	120.0 (0.0)
	PM3	120.0 (0.0)	120.0 (0.0)	120.0 (0.0)
	AM1/sparkle	120.0 (0.0)	120.0 (0.0)	120.0 (0.0)
NH_2				
distances	DFT	2.253	2.241	2.179
	PM3	2.257	2.253	2.167
	AM1/sparkle	2.200	2.211	2.196
angles	DFT	120.0 (0.1)	120.0 (0.1)	120.0 (0.1)
	PM3	114.4 (0.0)	117.3 (0.0)	120.0 (0.0)
	AM1/sparkle	120.0 (3.9)	120.0 (0.0)	120.0 (4.9)

[a] B3LYP/6-31G* and quasi-relativistic ECP of ref 84 for the lanthanide atom. [b] Ln−X distances are essentially equivalent in each complex. (In parentheses) unsigned mean deviation of bond angles.

However, for the lanthanide tricoordinated complexes (H, Me, F, Cl, Br, NH_2, Table 1) the ligand atoms were calculated using the 6-31G* basis set. Our semiempirical model in which the 4*f* electrons are placed in the core has been parametrized against DFT calculations in which the 4*f* electrons are also placed within the electronic core.

For each lanthanide, in addition to the 6 tricoordinated complexes (Table 1) we also selected up to 10 complexes from the CSD (Tables S2−S4, Figures S2−S4).[61] In line with the parametrization of the AM1/sparkle model, these complexes involved a range of coordinating ligands such as β-diketones, nitrates, mono-, bi-, tri-, and polydentate ligands.[60,63] We also chose at least one dilanthanide complex for each training set (Figures S2−S4). In view of the importance of the DOTA ligand (Chart 1) in MRI contrast agents we also included three structures involving the DOTA ligand within our training sets [A isomer with and without water and the IA isomer with water, Table 2]. The training sets for Eu, Gd, and Yb contained up to 19 reference structures. Each of the reference complexes was optimized at the DFT level, the structures of which are given in Tables 1, 2, and S2−S4. Our parametrization for the lanthanides thus differs from that for the AM1/sparkle model[60,63] in that our reference data are entirely calculated at the DFT level (rather than being obtained from crystal structures alone).

All semiempirical calculations were performed using our local semiempirical package (Manchester University Semi-Empirical, MUSE) program.[48] We have implemented the semiempirical method PM3 method including *d*-orbitals[46,47] and for comparison have also implemented the AM1/sparkle model[60] within our program and validated our algorithm against the available published data.[60,63] We note that for the location of minima on the potential energy surface, our program uses the GAUSSIAN 03[83] optimization suite, whereas the published AM1/sparkle model makes use of the optimization algorithms within the MOPAC suite of programs.[57]

3. Parametrization. Our initial goal was to obtain parameters for gadolinium. Stewart suggests that the two most common methods for generating initial sets of parameters are to use parameters from a previous method or to use values derived from a similar element.[45] In our case, neither of these approaches were possible due to the absence of either AM1 or PM3 published parameters for gadolinium. We also note that due to the different functional form of the AM1/sparkle model[60] and our orbital-based model we were unable to make use of the existing sparkle parameters for gadolinium for initial estimates of our core repulsion parameters.

The one-center terms, U_{ss}, U_{dd}, G_{ss}, G_{sd}, G_{dd}, and H_{sd}, were obtained by fitting these parameters (using a GA[85]) to the energies of 12 electronic states of the neutral and ionized gadolinium atom.[86] The parameter U_{pp} was also estimated from experimental data. Thus the one-center lanthanide parameters, where the 4*f* electrons are part of the electronic core can be obtained in essentially the same way as for first-row transition metals.[48] The remaining parameters (G_{pp}, β_s, β_p, β_d, ζ_s, ζ_p, ζ_d) were assigned different values for different parametrization runs. The core electron attraction and core repulsion parameters, ρ, δ_{Gd-X}, and α_{Gd-X}, were set equal to 1.0, 1.5, and 2.0. Importantly, in our approach *all* the semiempirical parameters were adjusted, with constraints placed upon individual parameters to prevent them from wandering toward unrealistic values, which may have limited their transferability. We note that even though we allowed the one-center terms U_{ss}, U_{dd}, G_{ss}, G_{sd}, G_{dd}, and H_{sd} to change from the GA optimized values, the relative energies of the different states of the neutral and charged gadolinium atom are in good agreement with experimental data (Table S5).

Table 2. Experimental and Calculated Average Distances (Å) and Dihedral Angles (deg) for the Lanthanide(III) DOTA Complexes

distance[a]	Eu[c]	Gd[d]	Yb
	DFT[b]		
Isomer A			
N	2.699	2.690	2.645
O	2.343	2.328	2.264
φ	39.4	39.5	40.2
Isomer IA + H_2O			
N	2.734 (2.680)	2.729 (2.663)	2.715[e]
O	2.381 (2.394)	2.365 (2.367)	2.298[e]
O (H_2O)	2.538 (2.480)	2.530 (2.463)	2.436[e]
φ	39.7 (38.7)	39.9 (38.5)	40.8[e]
Isomer IA + H_2O			
N	2.746	2.741	2.722
O	2.393	2.378	2.315
O (H_2O)	2.523	2.519	2.441
φ	−28.8	−29.1	−29.0
	PM3		
Isomer A			
N	2.697	2.700	2.645
O	2.384	2.359	2.284
φ	38.1	37.5	37.7
Isomer A + H_2O			
N	2.716	2.718	2.672
O	2.416	2.391	2.317
O (H_2O)	2.523	2.497	2.436
φ	38.3	37.7	37.7
Isomer IA + H_2O			
N	2.756	2.755	2.710
O	2.418	2.392	2.319
O (H_2O)	2.523	2.497	2.434
φ	−24.4	−23.0	−23.8
	AM1/Sparkle		
Isomer A			
N	2.603	2.617	2.525
O	2.389	2.397	2.325
φ	35.4	38.0	36.9
Isomer A + H_2O			
N	2.608	2.627	2.530
O	2.398	2.409	2.330
O (H_2O)	2.397	2.413	2.297
φ	36.1	38.6	36.7
Isomer IA + H_2O			
N	2.613	2.639	2.534
O	2.403	2.415	2.333
O (H_2O)	2.429	2.418	2.298
φ	−20.2	−22.4	−19.9

[a] φ is the twist angle between the basal plane occupied by four amine nitrogens and a capped plane occupied by the carboyxlate oxygens of the acetate arms. [b] B3LYP/3-21G and quasi-relativistic ECP of ref 84 for the lanthanide atom. [c] (In parentheses) average experimental values.[89] [d] (In parentheses) average experimental values.[90] [e] For comparison experimental values for the Lu structural parameters are N = 2.614 Å, O = 2.279 Å, O(H_2O) = 2.417 Å, and φ = 39.6°.[95]

Thus our parametrization scheme includes energetic data as well as structural data. We also note that our *s* and *p* Slater exponents (ξ_s, ξ_p) are quite close to those used in the INDO/S method for these lanthanides, whereas the Slater *d* exponents (ξ_d) are somewhat smaller than the corresponding INDO/S values (Table 3).[52]

Table 3. PM3 Parameters for Europium(III), Gadolinium(III), and Ytterbium(III)

parameter[a,b]	units	Eu	Gd	Yb
U_{ss}	eV	−18.826233	−18.911102	−18.650043
U_{pp}	eV	−7.389669	−7.242997	−7.350925
U_{dd}	eV	−20.425142	−20.259917	−19.196298
G_{ss}	eV	6.016223	6.053780	6.007332
G_{pp}	eV	6.583764	6.629378	6.637371
G_{dd}	eV	8.686045	8.771641	8.779865
G_{sd}	eV	6.539961	6.584258	6.593397
H_{sd}	eV	0.709285	0.620633	0.667674
β_s	eV	−7.731346	−7.592416	−7.727729
β_p	eV	−3.185841	−3.038541	−3.151070
β_d	eV	−5.068540	−4.952733	−4.988789
ξ_s	$bohr^{-1}$	1.481590	1.459057	1.459151
ξ_p	$bohr^{-1}$	1.655881	1.614106	1.649188
ξ_d	$bohr^{-1}$	1.748437	1.705403	1.826745
ρ	bohr	2.003400	1.704389	1.972353
δ_{Ln-H}	dimensionless	2.003450	2.058686	2.062443
δ_{Ln-C}	dimensionless	1.995470	2.041816	1.976463
δ_{Ln-N}	dimensionless	1.982809	1.921203	1.932329
δ_{Ln-O}	dimensionless	1.964953	1.909225	1.907816
δ_{Ln-F}	dimensionless	1.939396	1.971044	1.915106
δ_{Ln-S}	dimensionless	1.974976	2.126802	1.954339
δ_{Ln-Cl}	dimensionless	2.077221	2.061006	2.051176
δ_{Ln-Br}	dimensionless	2.077995	2.229090	2.142167
δ_{Ln-Ln}	dimensionless	3.959263	4.007627	3.969686
α_{Ln-H}	$Å^{-1}$	1.802290	1.823080	1.721239
α_{Ln-C}	$Å^{-1}$	1.767034	1.756414	1.744168
α_{Ln-N}	$Å^{-1}$	1.826384	1.864247	1.959332
α_{Ln-O}	$Å^{-1}$	1.886109	1.925632	1.977981
α_{Ln-F}	$Å^{-1}$	1.983411	2.090731	2.044649
α_{Ln-S}	$Å^{-1}$	1.869981	1.834960	1.947567
α_{Ln-Cl}	$Å^{-1}$	1.734821	1.770806	1.800099
α_{Ln-Br}	$Å^{-1}$	1.728463	1.731540	1.764436
α_{Ln-Ln}	$Å^{-1}$	1.556393	1.516730	1.558195

[a] For complexes containing B, δ_{Ln-B} and α_{Ln-B} were set equal to the corresponding values for C; for complexes containing P, δ_{Ln-P} and α_{Ln-P} were set equal to the corresponding values for N; for complexes containing Si, δ_{Ln-Si} and α_{Ln-Si} were set equal to the corresponding values for C. [b] For comparison INDO/S Slater exponents are as follows: ξ_s 1.656 (Eu), 1.678 (Gd), 1.812 $bohr^{-1}$ (Yb); ξ_p 1.448 (Eu), 1.463 (Gd), 1.549 $bohr^{-1}$ (Yb); ξ_d 2.229 (Eu), 2.243 (Gd), and 2.279 $bohr^{-1}$ (Yb).[52]

For gadolinium, each parametrization run involved the optimization of 33 parameters (including 18 bond specific terms) and a reference training set of 18 complexes, of which 7 contained more than 50 atoms. We carried out several parametrization runs starting from different initial parameter values, reference training sets, and weighting factors in the error function. Each explicit function and gradient calculation typically involved some 1200 SCF and force calculations, and due to the size of the reference structures the most time-consuming part of each SCF calculation was the transformation of the Cartesian forces (for each structure) into internal forces. Each parametrization run usually required less than 10 explicit gradient evaluations. In line with Stewart's algorithm[44,45] we also found that during the initial stages of the optimization the value of the error function (*S*, eq 7) dropped rapidly, partly due to the crude initial guess of the core repulsion parameters (ρ, δ_{Gd-X}, and α_{Gd-X}). The error

function evaluated using the final optimized parameters was typically less than 20% of the function evaluated using the initial parameters. The final gadolinium parameters are given in Table 3. It is worth pointing out that since our modified BFGS algorithm avoids explicit geometry optimization,[50,51] there is the possibility of obtaining parameters that yield very small gradients for the reference structures but that, upon geometry optimization, predict structures quite different from the reference ones. By including a relatively large number of reference structures and coordination environments we hope to minimize this effect (Tables S6−S8).

We found during our initial attempts to obtain lanthanide parameters for the $[Ln(DOTA)(OH_2)]^{1-}$complexes, that there was a tendency for the Ln−N distances to be overestimated by up to 0.2 Å, and for the dilanthanide complexes, the Ln−Ln distances were quite poorly predicted, deviating from the DFT values by up to 0.4 Å. These problems were somewhat overcome by scaling these internal coordinate gradients by quite large weighting factors relative to the other internal coordinate gradients (Table S1). Parameters for europium and ytterbium were obtained as follows. In line with Stewart's suggestion,[45] initial values for europium parameters were derived from the optimized gadolinium parameters but with the core repulsion parameters ρ, δ_{Gd-X}, and α_{Gd-X} reset to the values 1.0, 1.5, and 2.0. However, deriving the initial ytterbium parameters from those for gadolinium led to a set of parameters which yielded *d*-orbital populations that were too large to be consistent with the expected trends across the lanthanide series. Therefore the initial ytterbium parameters were extrapolated from the parameters of europium and gadolinium.

The final ytterbium parameters (Table 3) are quite close to the corresponding gadolinium ones, the largest change occurs for the ρ parameter which has increased by 16%, and, of the 32 optimized ytterbium parameters, only eight of these differ from the gadolinium ones by more than 5% (Table 3). Similarly, only three of the optimized ytterbium parameters differ by more than 5% from the europium ones, the largest difference being for the α_{Ln-N} parameter, which decreases by 7% (Table 3). Generally speaking, the observed parameter changes in going from Gd to Yb (separated by Tb, Dy, Ho, Er, and Tm) and also Eu to Yb appear to be quite small. Stewart[45] suggests interpolation or extrapolation as ways of obtaining initial estimates for parameters; given the closeness of the Yb parameters to those of Eu and Gd, extrapolation may be possible, without further optimization, to obtain parameters for other lanthanides close to the ones reported herein (e.g., Sm, Tb, Tm, Lu). However, it is important to recognize that the observed parameter changes may also be influenced not only by the properties of the elements themselves but also by the different training sets used (Tables S6−S8).

This parametrization strategy differs from our previous work in developing PM3 parameters for iron[50,51] in that we are able to obtain useful parameter sets without including data concerning the charges, spin densities, and $\langle S^2 \rangle$ value of the reference complexes. Moreover, we found that inclusion of the DFT atomic charges (scaling factor 2000 e^{-1}) did not significantly improve the final results. This was probably due to the fact that in our model our reference lanthanide complexes were all closed-shell. Importantly, the performance of our present approach with respect to any chosen molecular property can be tuned by a suitable adjustment of the weighting factors (Table S1).

Table 4. Average UME and UME_{Ln-X} (vs Experiment) for Complexes Used by Other Workers[60,63] in the AM1/Sparkle Parametrization of Europium, Gadolinium, and Ytterbium[a]

element[b]	DFT[c]	PM3[d]	AM1/sparkle[d]
europium (15)			
UME_{Ln-X}	0.0514	0.0607 (0.0588)	0.0767 (0.0673)
UME[e]	0.0982	0.1174 (0.1132)	0.1547 (0.1514)
gadolinium (15)			
UME_{Ln-X}	0.0587	0.0574 (0.0592)	0.0676 (0.0669)
UME[e]	0.1306	0.1198 (0.1141)	0.1532 (0.1584)
ytterbium (15)			
UME_{Ln-X}	0.0514	0.0516 (0.0630)	0.0653 (0.0835)
UME[e]	0.1247	0.0967 (0.0934)	0.1667 (0.2007)

[a] For individual UMEs and UME_{Ln-X} values refer to Tables S9−S11. [b] (In parentheses) number of complexes used for each element. [c] B3LYP/3-21G and quasi-relativistic ECP of ref 84 for the lanthanide atom. [d] (In parentheses) complexes calculated at the DFT level only. [e] Complexes containing more than one lanthanide atom were omitted: Eu (DOPCEQ, NUHIX and QECGOU); Gd (CULNIG10 and YAVSUJ); and Yb (NIJFER and XEWZOO).

The resulting parameters were then tested on a range of complexes not included in the reference training set to select those parameters giving the most balanced results. In line with our parametrization of iron[51] and the recently reported AM1* parametrization,[71] our goal in this work was to obtain sets of reasonable parameters which performed well for as many chemical applications as possible. As a result the final optimized parameters for Eu, Gd, and Yb (Table 3) do not necessarily correspond to those that yielded the lowest value of the error function. In this work we only report core repulsion parameters (δ_{Ln-X} and α_{Ln-X}) for complexes in our training set. However, for the large majority of lanthanide-(III) complexes in the CSD[61] the lanthanide ion is directly coordinated by either oxygen or nitrogen. Thus for atoms not directly coordinated to the lanthanide ion, for which we have not derived core repulsion parameters, the parameters of a closely related element can be used (e.g., for silicon use carbon etc., Table 3).

Computational Results

In order to measure the accuracy to which our model is capable of reproducing the reference structures, we have calculated the unsigned mean error (UME) for (i) the interatomic distances (R) between all the atoms of the coordination polyhedron (UME) and (ii) the interatomic distances (R) between the lanthanide central ion and the atoms directly coordinated to this atom (UME_{Ln-X}).[59] The UME (or UME_{Ln-X}) for any given structure (in Å) is calculated using eq 8

$$\mathrm{UME} = \frac{1}{n}\sum_{i=1}^{n} |R_{\mathrm{reference}} - R_{\mathrm{calculated}}| \qquad (8)$$

The *average* UME and UME_{Ln-X} are also reported for different sets of complexes (Tables 4, 5, and S6−S14).

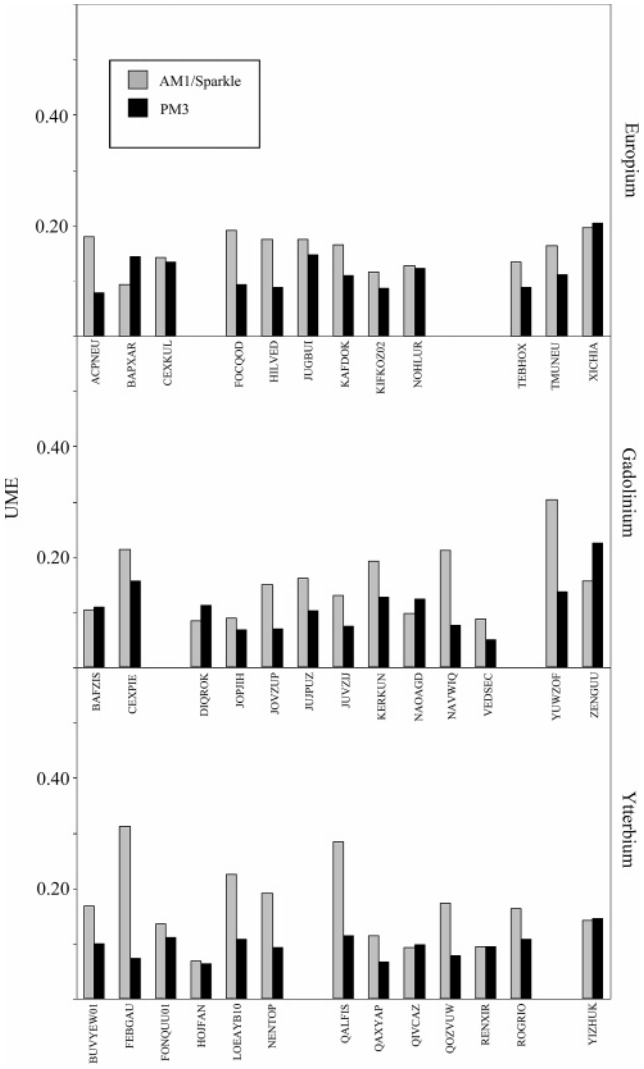

Figure 1. UME (Å) (vs experiment) for the complexes used by other workers[60,63] in the AM1/sparkle parametrization of europium, gadolinium, and ytterbium. Refer to Tables S9−S11 for individual UMEs. Complexes containing more than one lanthanide atom were omitted: Eu (DOPCEQ, NUXHIX, and QECGOU); Gd (CULNIG10 and YAVSUJ); and Yb (NIJFER and XEWZOO).

1. Calculation of Crystal Structures Using DFT. We have evaluated the performance of our chosen DFT method and the PM3 model in predicting the experimental structures (obtained from the CSD[61]) of complexes from the training sets used by other workers[60,63] in the parametrization of the AM1/sparkle model. For comparison we have also calculated these structures using our implementation of the AM1/sparkle method. The average UME and UME_{Ln-X} values for the europium, gadolinium, and ytterbium complexes are summarized in Table 4 and also Figure 1 (see also Tables S9−S11).[60,63]

Evidently, our chosen DFT method yields Ln−ligand distances close to the experimental values with UME_{Ln-X} of 0.0514, 0.0587, and 0.0514 Å for the europium, gadolinium, and ytterbium complexes, respectively (Table 4). Importantly for the prediction of crystal geometries, the average UME indicate that the PM3 model generally predicts structures a little closer to experiment for gadolinium and ytterbium than does the DFT method [Eu, 0.1132 (PM3), 0.0982 (DFT); Gd, 0.1141 (PM3), 0.1306 (DFT); Yb 0.0934 (PM3), 0.1247 Å (DFT)]. This finding is somewhat surprising given that the PM3 parameters were developed using DFT structures alone. Intuitively the quality of the PM3 structures should at best be as good as the DFT ones. The fact that PM3 predicts structures a little closer to experiment is likely to be due to a fortuitous cancellation of errors, probably as a result of the approximations inherent in the parameter optimization algorithm. One such approximation is that for each reference structure, the parameters are adjusted until the forces on the atoms of each structure are minimized, rather than performing explicit geometry optimization.

Table 5. Average UME and UME_{Ln-X} (vs DFT[a]) for Complexes in the Europium, Gadolinium, and Ytterbium PM3 Training Sets[b]

element[c]	AM1/sparkle[d]	PM3[d]
europium		
UME_{Ln-X}	0.1984 (0.1005)	0.0355 (0.0329)
UME[e]	0.2812 (0.1570)	0.0963 (0.0896)
gadolinium		
UME_{Ln-X}	0.1875 (0.0821)	0.0254 (0.0316)
UME[e]	0.2725 (0.1296)	0.0720 (0.0735)
ytterbium		
UME_{Ln-X}	0.1801 (0.0873)	0.0283 (0.0292)
UME[e]	0.2835 (0.1752)	0.0677 (0.0807)

[a] B3LYP/3-21G and quasi-relativistic ECP of ref 84 for the lanthanide atom. [b] For individual UME and UME_{Ln-X} values refer to Tables S6−S8. [c] (In parentheses) number of complexes used for each element. [d] (In parentheses) values *not* including LnX_3 (X = H, CH_3, Cl, F, Br, NH_2). [e] Complexes containing more than one lanthanide atom were omitted: Eu (DOPCEQ); Gd (ACAQGD01 and YAVSUJ); and Yb (XEWZOO).

The average UME values at the PM3 level for these structures [0.1174 (Eu), 0.1198 (Gd), 0.0967 Å (Yb)] are smaller than the corresponding AM1/sparkle values [0.1547 (Eu), 0.1532 (Gd), 0.1667 Å (Yb)] even though the PM3 model was parametrized to reproduce DFT gas-phase geometries and not crystal structures (Table 4). It would appear the PM3 model is a notable improvement over the existing AM1/sparkle model and can even rival DFT for accuracy in predicting the structures of various lanthanide crystal complexes. Figure 1 shows a plot of the UMEs (vs experiment) calculated for each of the europium, gadolinium, and ytterbium crystal structures. Overall the PM3 model generally gives smaller UMEs for the crystal structures than does the AM1/sparkle model. It is not surprising that the PM3 model is superior to the AM1/sparkle model given its increased flexibility due to the greater number of adjustable parameters. Importantly, despite the increase in the number of parameters for our PM3 model compared to the AM1/sparkle model[60] the actual increase in calculation time is negligible.

2. Calculation of Complexes in the PM3 Training Sets. We first discuss the average UME and UME_{Ln-X} for the PM3 and AM1/sparkle calculations for each PM3 training set (summarized in Table 5 and Figure 2; see also Tables S6−S8) to measure the accuracy to which they can reproduce the results of the DFT calculations. Figure 2 shows a plot of

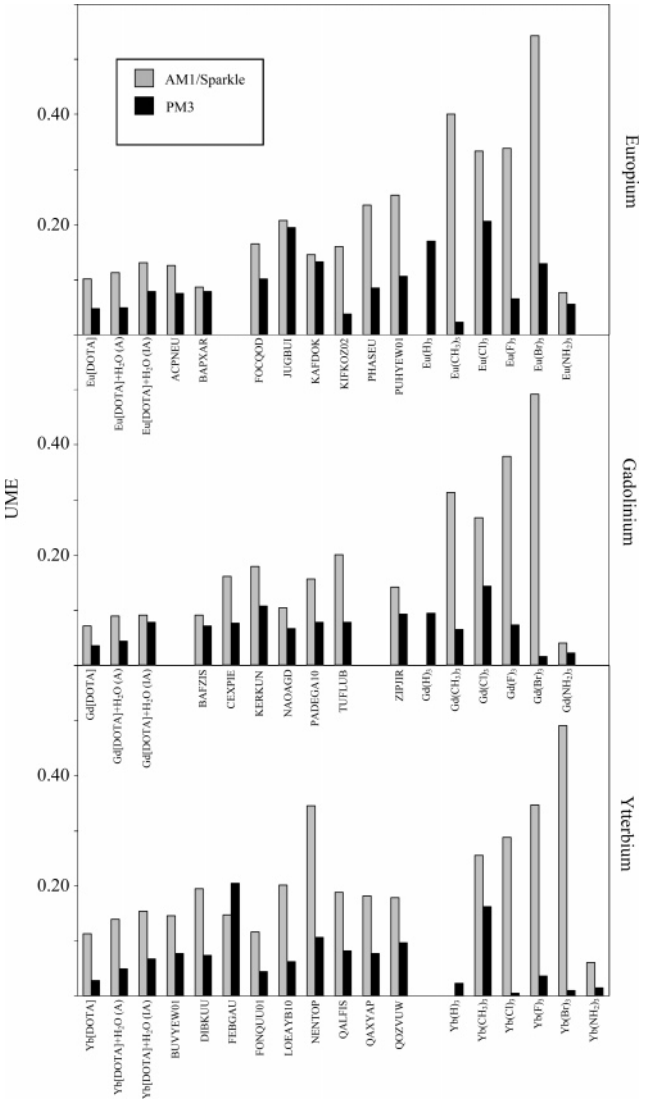

Figure 2. UME (Å) (vs DFT) for complexes in the europium, gadolinium, and ytterbium PM3 training sets. Refer to Tables S6−S8 for individual UMEs. Complexes containing more than one lanthanide atom were omitted: Eu (DOPCEQ); Gd (ACAQGD01 and YAVSUJ); and Yb (XEWZOO). AM1/sparkle UMEs for LnH_3 complexes were also omitted: Eu (1.3616 Å); Gd (1.5713 Å); and Yb (1.5625 Å).

the UMEs for each of the complexes in the europium, gadolinium, and ytterbium training sets. As expected the UMEs (vs DFT) for each structure are considerably smaller at the PM3 level than at the AM1/sparkle level. For each lanthanide, the average UME_{Ln-X} for each training set indicates the PM3 structures are very close to those at the DFT level [0.0355 (Eu), 0.0254 (Gd), and 0.0283 Å (Yb)]. Not surprisingly, the PM3 average UME_{Ln-X} are considerably better than those calculated using the AM1/sparkle parameters given that the AM1/sparkle model was parametrized to reproduce crystal structures [0.1984 (Eu), 0.1875 (Gd), 0.1801 Å (Yb)].[60,63] These findings are also reflected in the average UME_{Ln-X} when considering only the poly coordinated complexes (Table 5). The average UME (which reflects the ability of the semiempirical model to reproduce the geometry of the coordination polyhedron) are significantly smaller at the PM3 level [0.0963 (Eu), 0.0720 (Gd), 0.0677 Å (Yb)] than at the AM1/sparkle level [0.2812 (Eu), 0.2725 (Gd), 0.2835 Å (Yb)]. We turn now to discuss the complexes involving the DOTA ligand calculated using our new PM3 model.

Table 6. Relative Energies (kcal mol^{-1}) of the Complexes Involving the DOTA Ligand, Calculated at the DFT, AM1/Sparkle, and PM3 Levels of Theory

complex[b]	Eu	Gd	Yb
	DFT[a]		
$[Ln(DOTA)]^{1-}$ (A) + H_2O	0.0	0.0	0.0
$[Ln(DOTA)(OH_2)]^{1-}$ (A)	−42.7	−42.7	−40.7
$[Ln(DOTA)(OH_2)]^{1-}$ (IA)	−36.8	−36.7	−33.7
ΔE(A−IA)	−5.9	−6.0	−7.0
	PM3		
$[Ln(DOTA)]^{1-}$ (A) + H_2O	0.0	0.0	0.0
$[Ln(DOTA)(OH_2)]^{1-}$ (A)	−23.7	−31.2	−22.6
$[Ln(DOTA)(OH_2)]^{1-}$ (IA)	−21.4	−28.9	−17.6
ΔE(A−IA)	−2.3	−2.3	−5.0
	AM1/Sparkle		
$[Ln(DOTA)]^{1-}$ (A) + H_2O	0.0	0.0	0.0
$[Ln(DOTA)(OH_2)]^{1-}$ (A)	4.7	−17.8	−5.6
$[Ln(DOTA)(OH_2)]^{1-}$ (IA)	16.5	−6.6	6.1
ΔE(A−IA)	−11.8	−11.2	−11.7

[a] B3LYP/3-21G and quasi-relativistic ECP of ref 84 for the lanthanide atom. [b] ΔE is the relative energy of the A and IA isomers of $[Ln(DOTA)(OH_2)]^{1-}$.

$[Ln(DOTA)(OH_2)]^{1-}$ (Ln = Eu, Gd, or Yb). The mean Ln−ligand distances of the complexes involving the DOTA ligand calculated at the DFT (B3LYP), AM1/sparkle, and PM3 level along with the available experimental data are given in Table 2. The relative energies of the $[Ln(DOTA)(OH_2)]^{1-}$ isomers (A and IA) calculated at the DFT, AM1/sparkle, and PM3 levels are reported in Table 6.

It is now well understood that in solution $[Ln(DOTA)]^{-}$ complexes exist in two interconverting diasteromeric forms which differ in their arrangement of the acetate arms. For each form, the arrangement of the nitrogen and acetate oxygen atoms (which define two parallel squares) are twisted by an angle φ, yielding square antiprismatic (A) ($\varphi \sim 40°$) and inverted antiprismatic (IA) ($\varphi \sim -20°$) geometries. In solution the ninth coordination site is occupied by a single water molecule which undergoes rapid exchange with the surrounding bulk solvent and enhances the water proton relaxation rate.[87,88]

We first compare our DFT calculations with the available experimental data (Table 2).[89,90] Evidently, at the DFT level the Ln−N and the Ln−OH_2 distances are overestimated, whereas the Ln−O(DOTA) interactions are well-described at this level (Table 2). Previous calculations at the HF/3-21G level (46 + 4f^n ECP for lanthanides) have shown that for the $[Ln(DOTA)(OH_2)]^{1-}$ complex (Ln = La, Gd, Ho, Lu) there is a decrease in the calculated metal−ligand distances across the series coupled with a decrease in the stability of the nonacoordinated A isomer.[23] Thus our DFT structures of these complexes are in good agreement with the HF values in that there is a significant decrease in the metal−ligand distances from Eu through to Yb. For example, for the hydrated A isomer of the DOTA complex, the Ln−OH_2 distance decreases from 2.538 to 2.436 Å in going from

Eu to Yb (Table 2). In agreement with the calculations of Consentino et al. the Ln−O(DOTA) distances of the A isomer are predicted to be shorter than those of the IA isomer (Table 2).[23] Also, the general trend in increasing φ angles (Yb > Gd > Eu) for the nonacoordinated species reflects the decreasing ionic radius across the series leading to more compact structures (Table 2).

We turn now to the semiempirical calculations of the DOTA complexes. For each of the complexes (at both PM3 and AM1/sparkle level) the Ln−ligand distances decrease across the series as Eu > Gd > Yb. The PM3 Ln−OH_2 distances (isomer A) decrease going from Eu to Yb [2.523 (Eu), 2.497 (Gd), and 2.436 Å (Yb)] and are close to the corresponding values calculated at the DFT level (2.538, 2.530, 2.436 Å, Table 2). However, the AM1/sparkle Ln−OH_2 distances (A isomer) are less well predicted being ca. 0.1 Å shorter than the DFT values (Table 2). Similarly, the AM1/sparkle Ln−N distances for each structure are generally too short by some 0.1 Å or greater (Table 2).

As the ionic radius of the lanthanide cation decreases, the ninth coordination site at the metal center becomes less accessible; the structure around the ion becoming more compact. As a result the stability of the nonacoordinated species (isomers A and IA) should decrease, relative to the nonhydrated complex (isomer A).[23] This is indeed the trend predicted from the DFT calculations as the relative stability of the A and IA isomers decreases from −42.7 and −36.8 (Eu) to −40.7 and −33.7 (Yb) kcal mol^{-1}, respectively (Table 6). However, at both the PM3 and AM1/sparkle levels the trend is less clear. Evidently at the PM3 level the binding energies of the water molecules for the Eu, Gd, and Yb (isomer A) complexes (−23.7, −31.2, and −22.6 kcal mol^{-1}, Table 6) are much closer to the corresponding DFT values (−42.7, −42.7, and −40.7 kcal mol^{-1}) than for the AM1/sparkle model (4.7, −17.8, and −5.6 kcal mol^{-1}, Table 6). Overall, the PM3 estimates for the water-binding energies are quite poor and to achieve better estimates of energetic properties will probably require a greater number of energetic data in the fitting function, in line with our fitting function used to obtain parameters for iron.[51] Here, we note that the observed trend in our DFT calculations mirrors that of previous DFT studies (B3LYP/6-311G**) on a series of $[Ln(DOTA)(OH_2)]^{1-}$ complexes in which the water binding *free* energy decreases across a series as La > Gd > Ho > Lu (−3.84, −2.64, −0.81, and 0.20 kcal mol^{-1}).[23] Surprisingly, for this same series of complexes the Ln−OH_2 distances are found to also decrease as 2.635, 2.515, 2.462, and 2.424 Å, respectively (HF/3-21G in vacuo) in line with experiment.[23]

We finally note that the relative energies of the A and IA isomers at both the PM3 and AM1/sparkle levels are quite close to the corresponding DFT values (Table 6), although we find that the PM3 method underestimates and the AM1/sparkle model overestimates the relative stabilities (Table 6).

CSD Complexes. The UME and the UME_{Ln-X} values for each complex in the PM3 training sets are given in Tables S6−S8. The mean Ln−ligand bond distances for each complex are given in Tables S2−S4. Within each training set for Eu, Gd, and Yb there are a range of lanthanide coordination environments including β-diketone, nitrate, mono-, bi-, tri-, and polydentate ligands as well as dilanthanide complexes (Figures S2−S4). Each structure was obtained from the CSD[61] and optimized at the B3LYP/3-21G level using the quasi-relativistic $46 + 4f^n$ ECP of Dolg et al.[84] for the lanthanide atoms. We now compare structures both from the AM1/sparkle model and from our new PM3 model with those calculated at the DFT level.

Europium(III) Complexes. The training set for europium (Tables S2 and S6) involved 9 structures with up to decacoordination of the central Eu(III) ion (PHASEU and PUHYEW01); the largest complex containing 66 atoms (KAFDOK). At the PM3 level, the closest agreement between PM3 and DFT was found for the KIFKOZ02 complex (UME = 0.0381 Å, Table S6), whereas the largest discrepancy was calculated for the JUGBUI complex (UME = 0.1943 Å, Table S6). We find the europium−water oxygen distances are quite well predicted in the dieuropium complex [DOPCEQ, 2.534 (PM3), 2.501 Å (DFT), Table S2] and also in the complexes involving the terpyridine [PUHYEW01, 2.530 (PM3), 2.492 Å (DFT), Table S2] and trihydroxyhexane ligands [FOCQOD, 2.469 (PM3), 2.520 Å (DFT), Table S2]. Similarly, the europium−nitrate oxygen distances at the PM3 level are in satisfactory agreement with the DFT calculations [FOCQOD, JUGBUI, PHASEU, PUHYEW01, 2.492, 2.540, 2.550, 2.563 Å (PM3); 2.465, 2.493, 2.509, 2.574 Å (DFT), Table S2]. Finally we note that for the dieuropium complex involving bidentate acetate ligands (DOPCEQ), the Eu−Eu distance is somewhat underestimated at the PM3 level [3.852 Å (PM3), 3.983 Å (DFT), Table S2].

Gadolinium(III) Complexes. The training set for gadolinium (Tables S3 and S7) involved 9 structures with up to decacoordination of the central Gd(III) ion (PADEGA10); the largest complex containing 61 atoms (ZIPJIR). The smallest difference between the PM3 and DFT calculations is found for the complex involving oxydiacetate (NAOAGD, UME = 0.0665 Å, Table S7) ,while the largest discrepancy is calculated for the coordination polyhedron of the thiocyanate complex (KERKUN, UME = 0.1081 Å, Table S7). At the PM3 level the Gd−Gd distances in the two digadolinium complexes are predicted with varying degrees of success. In the complex involving primarily bidentate acetate ligands (ACAQGD01) the PM3 Gd−Gd distance differs from that of the DFT structure by 0.06 Å (Table S3), whereas in the complex involving the bridging nitrate ligands (YAVSUJ), the PM3 Gd−Gd is too short by some 0.16 Å (Table S3). The PM3 calculations of the complexes involving water mirror those of europium in that the gadolinium−water oxygen distances are well predicted at this level in a range of coordination environments (ACAQGD01, KERKUN, YAVSUJ, ZIPJIR, Table S3). Furthermore, the gadolinium−nitrogen distances are also well described in the BAFZIS, KERKUN, PADEGA10, and ZIPJIR complexes differing from the DFT values by 0.01−0.06 Å (Table S3).

Ytterbium(III) Complexes. The training set for ytterbium (Tables S4 and S8) involved 10 structures with up to

nonacoordination of the central Yb(III) ion; the largest complex contained some 98 atoms (XEWZOO). The largest discrepancy between the DFT and the PM3 structures occurs for the FEBGAU complex, the UME being 0.2041 Å (Table S8) which suggests a notable distortion of the coordination polyhedron at the PM3 level. The closest agreement with DFT is calculated for the complex involving the terpyridine ligand (FONQUU01, UME = 0.0446 Å, Table S8). Again, the Ln−water oxygen distances are quite well predicted at the semiempirical level in a range of different coordination environments [NENTOP, QALFIS, QOZVUW; 2.414, 2.410, 2.393 Å (PM3); 2.387, 2.366, 2.439 Å (DFT), Table S4]. Good agreement is also found in the ytterbium−nitrogen distances where the largest difference between DFT and PM3 is calculated for the LOEAYB10 complex, the PM3 values being on average some 0.06 Å longer than the DFT ones (Table S4). We note in the diytterbium complex (XEWZOO) the Yb−Yb distance is quite poorly predicted [4.234 (PM3), 4.623 Å (DFT), Table S4]. Such complexes are quite difficult to calculate accurately, given their large degree of conformational flexibility.

LnX_3 (Ln = Eu, Gd or Yb; X = H, Me, F, Cl, Br, or NH_2). There have been a number of theoretical studies of the lanthanide(III) trihalides which have sought to clarify the nature of the bonding, particularly the degree of covalent character in these species.[17,91,92,93] DFT calculations suggest the interaction is predominantly ionic especially for the lighter halogens and lanthanides, while for the more polarizable bromide or iodide there is some non-negligible ligand-to-metal charge transfer.[91]

The AM1/sparkle model has been parametrized primarily to reproduce structures of high coordination complexes, and therefore its ability to predict the geometries of low coordination complexes is not clear.[60,63] Since our goal in this work is to develop a completely general set of lanthanide parameters, we have also included a range of tricoordinated lanthanide(III) complexes in our training sets. Here, the use of the modified core repulsion function (eq 6)[45,50,51,70−72] allows for the fine-tuning of the structures where different atoms (other than nitrogen or oxygen) are directly coordinated to the lanthanide(III) ion. The structures of the tricoordinated lanthanide(III) complexes calculated at the DFT, AM1/sparkle, and PM3 level are given in Table 1. In Table S15, the *d*-orbital populations and charges (calculated at the DFT and PM3 level) for each of the tricoordinated complexes are also reported.

We first note that our DFT calculations are in good agreement with the calculations of Perrin et al. using the B3PW91 functional.[91] The hydride and alkyl complexes are strongly pyramidal and for fluoride a pyramidal structure is preferred, but for the heavier halides the complexes become increasingly planar. The calculations of Perrin et al.[91] suggest the Ln−X bond is predominantly ionic, and the pyramidalization of the complexes is related to the involvement of the valence *d* orbitals in the Ln−X bond. Therefore those complexes with the least population of the lanthanide *d* orbitals are found to be more pyramidal, while the increasing covalency with the heavier halides stabilizes the planar interactions through $d_\pi-p_\pi$ interactions.

The calculated Ln(III)−ligand distances are quite well reproduced at the PM3 level (Table 1), although we note that the trend of decreasing Ln(III)−X distances across the series (Eu to Yb) shown by DFT is not well defined; only for fluoride, chloride, and amide does the PM3 trend reflect that of the DFT calculations (Table 1). However, at the PM3 level the calculations correctly predict the hydride, alkyl, and fluoride complexes to be pyramidal, although the degree of pyramidalization is overestimated for hydride and fluoride complexes and underestimated for the alkyl complexes (Table 1). Evidently, despite these discrepancies, the PM3 model is a significant improvement over the AM1/sparkle model[60,63] which predicts all the structures to be trigonal planar. Clearly, the inclusion of atomic orbitals and the use of a modified core repulsion function has led to a significant improvement of the semiempirical description of these complexes. However, the trends in the *d* orbital occupations and atomic charges are less well reproduced (Table S15). For each ligand (H, Me, F, Cl, Br, NH_2) DFT predicts a decrease in the *d* orbital populations and an increase in the atomic charge moving from left to right across the lanthanide series (Eu, Gd, Yb). The trend in decreasing *d* orbital populations across the series (for each ligand) is essentially mirrored by the PM3 calculations even though the magnitude and trends in the atomic charges are quite different from the DFT calculations (Table S15). For the halides, the *d* orbital populations for any given lanthanide are calculated to be F < Cl < Br at the DFT level, whereas at the PM3 level this order is reversed. The inclusion and suitable weighting of the atomic charges and orbital occupations in the error function or the appropriate modification of the ligand atom parameters may help to alleviate this problem.

3. Calculation of Complexes not in the PM3 Training Sets. In the development of the AM1/sparkle model, each parameter set has been extensively tested in the calculation of a range of complexes from the CSD.[61] For this reason we decided to test our parameters for Eu, Gd, and Yb on up to 10 additional complexes (each optimized at the DFT level) from the CSD. We have therefore compared our PM3 calculations on a total of 28 (Eu), 28 (Gd), and 29 (Yb) complexes calculated at the DFT level, which we believe is sufficient to reflect a range of coordination environments. The UME for the additional complexes are given in Tables S12−S14. We can see that in general the agreement is extremely satisfactory.

For *all* Eu(III), Gd(III), and Yb(III) complexes considered herein, the average UME_{Ln-X} PM3 values for all interatomic distances between the lanthanide(III) ion and the ligand atoms of the first coordination sphere are 0.04, 0.03, and 0.03 Å, respectively (summarized in Table 7). These are smaller than the AM1/sparkle values of 0.09 Eu(III), 0.07 Gd(III), and 0.07 Yb(III), for their respective test sets. As far as the average UME are concerned (Table 7), the PM3 values are notably smaller (approximately half) than the corresponding AM1/sparkle values, which suggests the inclusion of lanthanide centered orbitals is important in describing the angular arrangement of ligands. We note that due to the computational expense of optimizing each of our test

Table 7. Comparison of the Average UME and UME_{Ln-X} (Å) for the PM3 and AM1/Sparkle Models

	Eu	Gd	Yb
PM3 (vs DFT[a])			
UME_{Ln-X}	0.04	0.03	0.03
UME[b]	0.10	0.09	0.07
structural comparisons	28	28	29
AM1/sparkle (vs CSD[c])			
UME_{Ln-X}	0.09[d]	0.07[d]	0.07[e]
UME	0.19[d]	0.18[d]	0.15[e]
structural comparisons	96[d]	70[d]	47[e]

[a] B3LYP/3-31G and quasi-relativistic ECP of ref 84 for the lanthanide atoms (6-31G* for the tricoordinated complexes). [b] Complexes containing more than one lanthanide atom were omitted: Eu (DOPCEQ); Gd (ACAQGD01 and YAVSUJ); and Yb (XEWZOO). [c] Cambridge Structural Database. [d] Reference 60. [e] Reference 63.

structures at the DFT level our test sets are smaller than those for the AM1/sparkle model.[60,63]

Conclusions

There are considerable difficulties in carrying out accurate "high level" DFT or ab initio calculations on lanthanide containing complexes. In particular, all-electron studies are generally prohibitive due to the large number of electrons and orbitals associated with the lanthanide atoms themselves; there are also difficulties in treating the 4*f* electrons and accounting for both relativistic effects and electron correlation. These problems have in part been addressed by the use of relativistic effective core potentials which incorporate relativistic effects into the core therefore reducing the computational effort for SCF calculations.[18] Further approximations can be made, such as the inclusion of the 4*f* electrons into the core, without significantly compromising the accuracy of the final results.

Semiempirical methods take these approximations much further. The AM1/sparkle model for lanthanides has been quite successful in describing a range of highly coordinated lanthanide complexes.[60,63] The sparkle model relies on the fact that for many lanthanide complexes the Ln−ligand bonds are largely electrostatic in nature. While the approximations in such a model appear to be quite severe, the AM1/sparkle model does quite well in predicting the coordination polyhedron of various lanthanide(III) complexes. Since the sparkle model assumes complete ionization of the valence electrons, covalent effects which may in some complexes be non-negligible cannot be included. Therefore in this work we have sought to build upon the suggestion by Freire et al. that covalent effects could be accounted for in semiempirical sparkle calculations by the inclusion of a set of orbitals on the sparkle atom.[60] Thus our PM3 model takes the approximations inherent in a DFT/RECP calculation further, but the approximations used are less severe compared to the AM1/sparkle approach.

Although semiempirical MO methods are formally minimal basis methods, we find that our parametrized PM3 model is generally comparable to DFT calculations using a 3-21G basis and the quasi-relativistic core potential of Dolg et al.[84] for the complexes calculated herein. The closeness of the PM3 results to the DFT calculations indicates we have been quite successful in developing a model and an appropriate parametrization strategy for obtaining semiempirical parameters for trivalent lanthanide complexes. Furthermore, our model is also shown to be essentially superior to the AM1/sparkle model for predicting crystal structures even though our model has been parametrized to reproduce DFT calculations. This is not surprising in view of the flexibility resulting from the number of adjustable parameters included in the PM3 model. We have sought to obtain a parameter set that will allow a large range of lanthanide(III)−ligand interactions to be considered. The results presented here show that in general we have been quite successful in being able to predict the structural and to a lesser extent the more demanding energetic quantities of theses species. We could, most probably, achieve greater accuracy by including a larger number of energetic reference data in our training sets, a larger training set, and possibly obtaining initial one-center parameters for europium and ytterbium directly from experimental data rather than using the gadolinium parameters for initial estimates. As with DFT calculations using RECPs, a given semiempirical core is only likely to be valid for a given formal oxidation state of the lanthanide atom.[94] Therefore the current model may not be successful in describing processes which involve a change in the formal oxidation state of the lanthanide. However, we believe the parameter set presented here would represent a good starting point for further refinement of the PM3 model for the elements (Eu, Gd, Yb) reported herein and the remaining lanthanide metals.

Acknowledgment. We thank EPSRC for support of this work and Dr. James J. P. Stewart for helpful discussions.

Supporting Information Available: Tables S1−S15, Figures S1−S4, and the Cartesian coordinates of all CSD[61] structures and DOTA complexes optimized at the DFT level. This material is available free of charge via the Internet at http://pubs.acs.org.

References

(1) Bouno-Core, G. E.; Li, H.; Marciniak, B. *Coord. Chem. Rev.* **1990**, *99*, 55.

(2) de Sá, G. F.; Malta, O. L.; de Mello Donegá, C.; Simas, A. M.; Longo, R. L.; Santa-Cruz, P. A.; da Silva, E. F., Jr. *Coord. Chem. Rev.* **2000**, *196*, 165.

(3) Parker, D.; Dickins, R. S.; Puschmann, H.; Crossland, C.; Howard, J. A. K. *Chem. Rev.* **2002**, *102*, 1977.

(4) Kido, J.; Okamoto, Y. *Chem. Rev.* **2002**, *102*, 2357.

(5) Lauffer, R. B. *Chem. Rev.* **1987**, *87*, 901.

(6) Choppin, G. R.; Schaab, K. M. *Inorg. Chim. Acta* **1996**, *252*, 299.

(7) Aime, S.; Botta, M.; Fasano, M.; Terreno, E. *Chem. Soc. Rev.* **1998**, *27*, 19.

(8) Thunus, L.; Lejeune, R. *Coord. Chem. Rev.* **1999**, *184*, 125.

(9) Caravan, P.; Ellison, J. J.; McMurry, T. J.; Lauffer, R. B. *Chem. Rev.* **1999**, *99*, 2293.

(10) DOTA = 1,4,7,10-tetraaza-1,4,7,10-tetrakis(carboxymethyl) cyclododecane.

(11) OECD/NEA. *Actinide and Lanthanide Product Partitioning and Transmutation*; Proceedings of the Fifth Information Exchange Meeting, Mol, Belgium, November 25−27, 1998.

(12) OECD/NEA. *Actinide and Fission Product Partitioning and Transmutation*; Proceedings of the Seventh Information Exchange Meeting, Jeju, Republic of Korea, October 14−16, 2002.

(13) Morgado, C. A.; McNamara, J. P.; Hillier, I. H.; Sundararajan, M. *Mol. Phys.* **2005**, *103*, 905.

(14) Sundararajan, M.; Hillier, I. H.; Burton, N. A *J. Phys. Chem. A* **2006**, *110*, 785.

(15) Sundararajan, M.; Surendren, R. A.; Hillier, I. H. *Chem. Phys. Lett.* **2005**, *418*, 92.

(16) Villa, A.; Cosentino, U.; Pitea, D.; Moro, G.; Maiocchi, A. *J. Phys. Chem. A* **2000**, *104*, 3421.

(17) Cundari, T. R.; Sommerer, S. O.; Strohecker, L. A.; Tippett, L. *J. Chem. Phys.* **1995**, *103*, 7058.

(18) Maron, L.; Eisenstein, O. *J. Phys. Chem. A* **2000**, *104*, 7140.

(19) Cao, X.; Dolg, M. *Chem. Phys. Lett.* **2001**, *349*, 489.

(20) Cao, X.; Dolg, M. *Mol. Phys.* **2003**, *101*, 1967.

(21) Cao, X.; Dolg, M. *J. Theor. Comput. Chem.* **2005**, *4*, 583.

(22) Takeda, K.; Tsuchiya, T.; Nakano, H.; Taketsugu, T.; Hirao, K. *J. Mol. Struct. (Theochem)* **2001**, *537*, 107.

(23) Cosentino, U.; Villa, A.; Pitea, D.; Moro, G.; Barone, V.; Maiocchi, A. *J. Am. Chem. Soc.* **2002**, *124*, 4901.

(24) Cosentino, U.; Moro, G.; Pitea, D.; Calabi, L.; Maiocchi, A. *J. Mol. Struct. (Theochem)* **1997**, *392*, 75.

(25) Smentek, L.; Hess, B. A.; Cross, J. P.; Manning, H. C.; Bornhop, D. J. *J. Chem. Phys.* **2005**, *123*, 244302.

(26) Girichev, G. V.; Giricheva, N. I.; Haaland, A.; Kuzmina, N. P.; Samdal, S.; Strenalyuk, T. N.; Tverdova, N. V.; Zaitseva, I. G. *Inorg. Chem.* **2006**, *45*, 5179.

(27) Guillaumont, D. *J. Phys. Chem. A* **2004**, *108*, 6893.

(28) Cao, X.; Dolg, M. *Mol. Phys.* **2003**, *101*, 2427.

(29) Heiberg, H.; Gropen, O.; Laerdahl, J. K.; Swang, O.; Wahlgren, U. *Theor. Chem. Acc.* **2003**, *110*, 118.

(30) Cundari, T. R. *J. Chem. Soc., Dalton Trans.* **1998**, 2771.

(31) Fossheim, R.; Dugstad, H.; Dahl, S. G. *Eur. J. Med. Chem.* **1995**, *30*, 539.

(32) THP = 1,4,7,10-tetrakis (2-hydroxypropyl)-1,4,7,10-tetraazacyclododecane; TMA = 1,4,7,10-tetrakis[(*N*-methylcarbamoyl)methyl]-1,4,7,10-tetraazacyclododecane; DOTMP = 1,4,7,10-tetraazacyclododecane-1,4,7,10-tetrakis(methylenemethylphosphinate).

(33) Cosentino, U.; Moro, G.; Pitea, D.; Villa, A.; Fantucci, P. C.; Maiocchi, A.; Uggeri, F. *J. Phys. Chem. A* **1998**, *102*, 4606.

(34) Kowall, T.; Foglia, F.; Helm, L.; Merbach, A. E. *J. Am. Chem. Soc.* **1995**, *117*, 3790.

(35) van Veggel, C. J. M.; Reinhoudt, D. N. *Chem. Eur. J.* **1999**, *5*, 90.

(36) Field, M. J.; Basch, M.; Karplus, M. *J. Comput. Chem.* **1990**, *11*, 700.

(37) Gao, J.; Xia, X. *Science* **1992**, *258*, 631.

(38) Maseras, F.; Morokuma, K. *J. Comput. Chem.* **1995**, *16*, 1170.

(39) Tresadern, G.; Wang, H.; Faulder, P. F.; Burton, N. A.; Hillier, I. H. *Mol. Phys.* **2003**, *101*, 2775.

(40) Alhambra, C.; Luz Sanchez, M.; Corchado, J.; Gao, J.; Truhlar, D. G. *Chem. Phys. Lett.* **2001**, *347*, 512.

(41) Rossi, I.; Truhlar, D. G. *Chem. Phys. Lett.* **1995**, *233*, 231.

(42) Dewar, M. J. S.; Thiel, W. *J. Am. Chem. Soc.* **1977**, *99*, 4899.

(43) Dewar, M. J. S.; Zoebisch, E. G.; Healy, E. F.; Stewart, J. J. P. *J. Am. Chem. Soc.* **1993**, *115*, 5348.

(44) Stewart, J. J. P. *J. Comput. Chem.* **1989**, *10*, 209.

(45) Stewart, J. J. P. *J. Mol. Model.* **2004**, *10*, 155.

(46) Thiel, W.; Voityuk, A. A. *Theor. Chim. Acta* **1992**, *81*, 391.

(47) Thiel, W.; Voityuk, A. A. *Theor. Chim. Acta* **1996**, *93*, 315.

(48) Mohr, M.; McNamara, J. P.; Wang, H.; Rajeev, S. A.; Ge, J.; Morgado, C.; Hillier, I. H. *Faraday Discuss.* **2003**, *124*, 413.

(49) Sundararajan, M.; McNamara, J. P.; Hillier, I. H.; Wang, H.; Burton, N. A. *Chem. Phys. Lett.* **2005**, *404*, 9.

(50) McNamara, J. P.; Sundararajan, M.; Hillier, I. H. *J. Mol. Graphics Modell.* **2005**, *24*, 128.

(51) McNamara, J. P.; Sundararajan, M.; Hillier, I. H., Ge, J.; Campbell, A.; Morgado, C. *J. Comput. Chem.* **2006**, *27*, 1307.

(52) Culberson, J. C.; Knappe, P.; Rösch, N.; Zerner, M. C. *Theor. Chim. Acta* **1987**, *71*, 21.

(53) Kotzian, M.; Rösch, N. *J. Phys. Chem.* **1992**, *96*, 7288.

(54) Kotzian, M.; Rösch, N.; Zerner, M. C. *Theor. Chim. Acta* **1992**, *81*, 201.

(55) Kotzian, M.; Rösch, N. *J. Mol. Spectrosc.* **1991**, *147*, 346.

(56) Stewart, J. J. P. *J. Comput.-Aided Mol. Des.* **1990**, *4*, 1.

(57) Stewart, J. J. P. *MOPAC 2000 Manual*; Fujitsu Ltd.: 1999. http://home.att.net/~mopacmanual (accessed September 2006).

(58) de Andrade, A. V. M.; da Costa, N. B., Jr.; Simas, A. M.; de Sá, G. F. *Chem. Phys. Lett.* **1994**, *227*, 349.

(59) Rocha, G. B.; Freire, R. O.; da Costa, N. B, Jr.; de Sá, G. F.; Simas, A. M. *Inorg. Chem.* **2004**, *13*, 2346.

(60) Freire, R. O.; Rocha, G. B.; Simas, A. M. *Inorg. Chem.* **2005**, *44*, 3299.

(61) Allen, F. H. *Acta Crystallogr., Sect. B: Struct. Sci.* **2002**, *58*, 380.

(62) Freire, R. O.; da Costa, N. B., Jr.; Rocha, G. B.; Simas, A. M. *J. Chem. Theor. Comput.* **2006**, *2*, 64.

(63) Freire, R. O.; Rocha, G. B.; Simas, A. M. *J. Comput. Chem.* **2005**, *26*, 1524.

(64) Freire, R. O.; da Costa, N. B., Jr.; Rocha, G. B.; Simas, A. M. *J. Phys. Chem. A* **2006**, *110*, 5897.

(65) da Costa, N. B., Jr.; Freire, R. O.; Rocha, G. B.; Simas, A. M. *Inorg. Chem. Commun.* **2005**, *8*, 831.

(66) Freire, R. O.; da Costa, N. B., Jr.; Rocha, G. B.; Simas, A. M. *J. Organomet. Chem.* **2005**, *690*, 4099.

(67) Bastos, C. C.; Freire, R. O.; Rocha, G. B.; Simas, A. M. *J. Photochem. Photobiol., A* **2006**, *177*, 225.

(68) Freire, R. O.; do Monte, E. V.; Rocha, G. B.; Simas, A. M. *J. Organomet. Chem.* **2006**, *691*, 2584.

(69) Freire, R. O.; Rocha, G. B.; Simas, A. M. *Chem. Phys. Lett.* **2006**, *425*, 138.

(70) Voityuk, A. A.; Rösch, N. *J. Phys. Chem. A* **2000**, *104*, 4089.

(71) Winget, P.; Horn, A. H. C.; Selçuki, C.; Martin, B.; Clark, T. *J. Mol. Model.* **2003**, *9*, 408.

(72) Winget, P.; Clark, T. *J. Mol. Model.* **2005**, *11*, 439.

(73) Cundari, T. R.; Deng, J.; Fu. W. *Int. J. Quantum Chem.* **2000**, *77*, 421.

(74) Sundararajan, M.; McNamara, J. P.; Mohr, M.; Wang, H.; Hillier, I. H. *Biochem. Soc. Trans.* **2005**, *33*, 20.

(75) Brothers, E. N.; Merz, K. M., Jr. *J. Phys. Chem. B* **2002**, *106*, 2779.

(76) Hutter, M. C.; Reimers, J. R.; Hush, N. S. *J. Phys. Chem. B* **1998**, *102*, 8080.

(77) Stewart, J. J. P. *J. Comput. Chem.* **1989**, *10*, 221.

(78) Stewart, J. J. P. *J. Comput. Chem.* **1991**, *12*, 320.

(79) Becke, A. D. *J. Chem. Phys.* **1993**, *98*, 5648.

(80) Miehlich, B.; Savin, A.; Stoll, H.; Preuss, H. *Chem. Phys. Lett.* **1989**, *157*, 200.

(81) Lee, C.; Yang, W.; Parr, R. G. *Phys. Rev. B* **1988**, *37*, 785.

(82) Frisch, K.-M.; Trucks, G. W.; Schlegel, H. B.; Scuseria, G. E.; Robb, M. A.; Cheeseman, J. R.; Zakrzewski, V. G.; Montgomery, J. A., Jr.; Stratmann, R. E.; Burant, J. C.; Dapprich, S.; Millam, J. M.; Daniels, A. D.; Kudin, K. N.; Strain, M. C.; Farkas, O.; Tomasi, J.; Barone, V.; Cossi, M.; Cammi, R.; Mennucci, B.; Pomelli, C.; Adamo, C.; Clifford, S.; Ochterski, J.; Petersson, G. A.; Ayala, P. Y.; Cui, Q.; Morokuma, K.; Malick, D. K.; Rabuck, A. D.; Raghavachari, K.; Foresman, J. B.; Cioslowski, J.; Ortiz, J. V.; Stefanov, B. B.; Liu, G.; Liashenko, A.; Piskorz, P.; Komaromi, I.; Gomperts, R.; Martin, R. L.; Fox, D. J.; Keith, T.; Al-Laham, M. A.; Peng, C.-Y.; Nanayakkara, A.; Gonzalez, C.; Challacombe, M.; Gill, P. M. W.; Johnson, B. G.; Chen, W.; Wong, M. W.; Andres, J. L.; Head-Gordon, M.; Replogle E. S.; Pople, J. A. *Gaussian 98*, *Revision A.7*; Gaussian Inc.: Pittsburgh, PA, 1998.

(83) Frisch, M. J.; Trucks, G. W.; Schlegel, H. B.; Scuseria, G. E.; Robb, M. A.; Cheeseman, J. R.; Montgomery, J. A., Jr.; Vreven, T.; Kudin, K. N.; Burant, J. C.; Millam, J. M.; Iyengar, S. S.; Tomasi, J.; Barone, V.; Mennucci, B.; Cossi, M.; Scalmani, G.; Rega, N.; Petersson, G. A.; Nakatsuji, H.; Hada, M.; Ehara, M.; Toyota, K.; Fukuda, R.; Hasegawa, J.; Ishida, M.; Nakajima, T.; Honda, Y.; Kitao, O.; Nakai, H.; Klene, M.; Li, X.; Knox, J. E.; Hratchain, H. P.; Cross, J. B.; Bakken, V.; Adamo, C.; Jaramillo, J.; Gomperts, R.; Stratmann, R. E.; Yazyev, O.; Austin, A. J.; Cammi, R.; Pomelli, C.; Ochterski, J. W.; Ayala, P. Y.; Voth, G. A.; Salvador, P.; Dannenberg, J. J.; Zakrzewski, V. G.; Dapprich, S.; Daniels, A. D.; Strain, M. C.; Farkas, O.; Malick, D. K.; Rabuck, A. D.; Raghavachari, K.; Foresman, J. B.; Ortiz, J. V.; Cui, Q.; Baboul, A. G.; Clifford, S.; Cioslowski, J.; Stefanov, B. B.; Liu, G.; Liashenko, A.; Piskorz, P.; Komaromi, I.; Martin, R. L.; Fox, D. J.; Keith, T., Al-Laham, A.; Peng, C. Y.; Nanayakkara, A.; Challacombe, M.; Gill, P. M. W.; Johnson, B.; Chen, W.; Wong, M. W.; Gonzalez, C.; Pople, J. A. *Gaussian 03*, *Revision C.02*; Gaussian, Inc.: Wallingford, CT, 2004.

(84) Dolg, M.; Stoll, H.; Savin, A.; Preuss, H. *Theor. Chim. Acta* **1989**, *75*, 173.

(85) Levine, D. *PGAPack*, *Version 1.0*; Mathematics and Computer Science Division Argonne National Laboratory: Argonne, IL, 1995.

(86) Ralchenko, Y.; Jou, F.-C.; Kelleher, D. E.; Kramida, A. E.; Musgrove, A.; Reader, J.; Wiese, W. L.; Olsen, K. *NIST Atomic Spectra Database*, *Version 3.1.0*; National Institute of Standards and Technology: Gaithersburg, MD, September 4, 2006.

(87) Aime, S.; Botta, M.; Fasano, M.; Terreno, E. *Acc. Chem. Res.* **1999**, *32*, 941.

(88) Botta, M. *Eur. J. Inorg. Chem.* **2000**, 399.

(89) Spirelet, M. R.; Rebizant, J.; Desreux, J. F.; Loncin, M. F. *Inorg. Chem.* **1984**, *23*, 359.

(90) Kumar, K.; Allen, Chang, C.; Francesconi, L. C.; Dischino, D. D.; Malley, M. F.; Gougoutas, J. Z.; Tweedle, M. F. *Inorg. Chem.* **1994**, *33*, 3567.

(91) Perrin, L.; Maron, L.; Eisenstein, O. *Faraday Discuss.* **2003**, *124*, 25.

(92) Adamo, C.; Maldivi, P. *J. Phys. Chem. A.* **1998**, *102*, 6812.

(93) Lanza, G.; Fragalà, I. L. *Chem. Phys. Lett.* **1996**, *255*, 341.

(94) Eisenstein, O.; Maron, L. *J. Organomet. Chem.* **2002**, *647*, 190.

(95) Aime, S.; Barge, A.; Botta, M.; Fasano, M.; Ayala, J. D.; Bombieri, G. *Inorg. Chem. Acta* **1996**, *246*, 423.

CT600304G